[CANCER RESEARCH 61, 687–693, January 15, 2001]

Glucagon-like Peptide (GLP)-2 Reduces Chemotherapy-associated Mortality and Enhances Cell Survival in Cells Expressing a Transfected GLP-2 Receptor[1]

Robin P. Boushey, Bernardo Yusta, and Daniel J. Drucker[2]

Department of Medicine, University Health Network, Toronto General Hospital [D. J. D.], and Banting and Best Diabetes Centre [R. P. B., B. Y.], University of Toronto, Toronto, Ontario, M5G 2C4 Canada

ABSTRACT

Chemotherapeutic agents produce cytotoxicity via induction of apoptosis and cell cycle arrest. Rapidly proliferating cells in the bone marrow and intestinal crypts are highly susceptible to chemotherapy, and damage to these cellular compartments may preclude maximally effective chemotherapy administration. Glucagon-like peptide (GLP)-2 is an enteroendocrine-derived regulatory peptide that inhibits crypt cell apoptosis after administration of agents that damage the intestinal epithelium. We report here that a human degradation-resistant GLP-2 analogue, h[Gly2]-GLP-2 significantly improves survival, reduces bacteremia, attenuates epithelial injury, and inhibits crypt apoptosis in the murine gastrointestinal tract after administration of topoisomerase I inhibitor irinotecan hydrochloride or the antimetabolite 5-fluorouracil. h[Gly2]-GLP-2 significantly improved survival and reduced weight loss but did not impair chemotherapy effectiveness in tumor-bearing mice treated with cyclical irinotecan. Furthermore, h[Gly2]-GLP-2 reduced chemotherapy-induced apoptosis, decreased activation of caspase-8 and -3, and inhibited poly(ADP-ribose) polymerase cleavage in heterologous cells transfected with the GLP-2 receptor. These observations demonstrate that the antiapoptotic effects of GLP-2 on intestinal crypt cells may be useful for the attenuation of chemotherapy-induced intestinal mucositis.

INTRODUCTION

Chemotherapeutic agents exert their cytoablative actions on rapidly proliferating cells via several different mechanisms, ultimately leading to cell cycle arrest and/or cellular apoptosis. The cytotoxic actions of chemotherapeutic agents are not tumor specific, and injury to normal cells in the bone marrow and intestinal crypt often complicates the treatment of patients with neoplastic disease (1, 2). Although molecules such as granulocyte-colony stimulating factor may be used to attenuate bone marrow toxicity after chemotherapy (3), no agents are currently available that selectively prevent chemotherapy-induced cell death in the intestinal crypt compartment. As a result, gastrointestinal toxicity characterized by severe mucositis and diarrhea often limits both the dose and duration of chemotherapy treatment, leading to reduced treatment effectiveness in susceptible patients.

Several intestine-derived molecules have been identified that maintain the integrity of the mucosal epithelium in part via prevention of apoptosis after intestinal injury. For example, intestinal trefoil factor promotes resistance to apoptosis after cellular injury *in vitro* (4), and intestinal trefoil factor-deficient mice exhibit enhanced susceptibility to intestinal injury and increased colonic epithelial cell apoptosis *in vivo* (5). Similarly, keratinocyte growth factor protects mice from chemotherapy and radiation-induced intestinal injury (6), and fibroblast growth factor 2, transforming growth factor β, cytokines, interleukin 11, and interleukin 15 reduce intestinal apoptosis *in vivo* (7–10).

GLP-2[3] is an intestinotrophic peptide secreted by enteroendocrine cells in response to intestinal injury (11–13). Exogenous administration of GLP-2 is trophic to the small and large intestinal epithelium in part via stimulation of crypt cell proliferation (14). Administration of GLP-2 to rodents with indomethacin-induced intestinal injury improves survival and reduces epithelial damage in part via inhibition of apoptosis in the crypt compartment (15). The antiapoptotic actions of GLP-2 prompted us to examine whether GLP-2 might ameliorate the extent of intestinal injury arising from chemotherapy administration *in vivo*.

MATERIALS AND METHODS

Materials

5-FU was obtained from Roche Laboratories. IRT (7-ethyl-10-[4-(1-piperidino)-1-piperidino]carbonyloxycamptothecin) used in mice was a gift from Pharmacia Upjohn (Mississauga, Canada), and recombinant h[Gly2]-GLP-2 was kindly provided by NPS Allelix Corp. (Mississauga, Canada). Cell culture experiments were performed using IRT and forskolin obtained from Sigma (St. Louis, MO).

Animals

All experimental protocols were approved by the Animal Care Committee of the University Health Network–Toronto General Hospital. Experiments with IRT alone were performed in 8–9-week-old CD1 female mice (Charles River, Toronto, Canada). Experiments with 5-FU were carried out in 11–13-week-old BDF-1 female mice (Harlan, Toronto, Canada). Experiments using IRT treatment in BALB/c mice inoculated with CT-26 murine colon carcinoma cells were performed in 10-week-old female mice (Charles River). All mice were housed in plastic-bottomed wire-lid cages and maintained on a 12-h light/12-h dark cycle in a temperature-controlled room and given water and chow *ad libitum*.

Experimental Protocols

For all animal experiments, mice received s.c. injection of either 0.5 ml of saline (PBS) or 10 μg of h[Gly2]-GLP-2, a human GLP-2 analogue (12) dissolved in 0.5 ml of saline, twice daily at 8 a.m. and 6 p.m. beginning 3 days before administration of either 5-FU (400 mg/kg) or IRT (280 mg/kg). For non-tumor-bearing mice, studies were carried out in adult CD1 female mice. For tumor-bearing BALB/c mice, CT-26 murine colon carcinoma cells (American Tissue Culture Collection) syngeneic to BALB/c mice were grown in monolayer cultures in DMEM (4.5 grams/liter glucose) supplemented with 5% FCS, 1 mM pyruvate (Life Technologies, Inc., Burlington, Canada), and penicillin G sodium (100 units/ml)/streptomycin sulfate (0.1 mg/ml; Sigma) in a humidified 5% CO_2 atmosphere at 37°C as described previously (16). A single cell suspension with >90% viability was injected s.c. (5×10^5 cells) in the left flank region. Six days later, a 7-day treatment regimen was initiated [3 days of treatment with either 0.5 ml of saline (PBS) or 10 μg of h[Gly2]-

Received 6/26/00; accepted 11/13/00.

The costs of publication of this article were defrayed in part by the payment of page charges. This article must therefore be hereby marked *advertisement* in accordance with 18 U.S.C. Section 1734 solely to indicate this fact.

[1] This work was supported in part by grants from the Medical Research Council of Canada and the Ontario Research and Development Challenge Fund. R. P. B. is a research fellow and D. J. D. is a Senior Scientist of the Medical Research Council of Canada. GLP-2 is the subject of a licensing agreement between the University of Toronto, Toronto General Hospital, D. J. D., and NPS Pharmaceuticals Corp., and D. J. D. is a consultant to NPS Pharmaceuticals Corp.

[2] To whom requests for reprints should be addressed, at University Health Network–Toronto General Hospital, 200 Elizabeth Street CCRW 3-838, Toronto, Ontario, M5G 2C4 Canada. Phone: (416) 340-4125; Fax: (416) 978-4108; E-mail: d.drucker@utoronto.ca.

[3] The abbreviations used are: GLP, glucagon-like peptide; PARP, poly(ADP-ribose) polymerase; IR, inhibition ratio; TUNEL, terminal deoxynucleotidyl transferase-mediated nick end labeling; BHK, baby hamster kidney; pNA, paranitroanilide; 5-FU, 5-fluorouracil; IRT, irinotecan.

GLP-2 administered s.c. twice daily at 8 a.m. and 6 p.m., followed by a 3-day regimen of IRT (100 mg/kg dose) or vehicle administered via the i.p. route once daily and a 24-h recovery period]. This 7-day regimen was repeated three times ($n = 25$ mice/group), at which point some animals in the control groups became moribund; hence, all mice were euthanized after receiving CO_2 anesthesia 30 days after tumor implantation. The tumor IR was determined using the following equation: IR (%) = $(1 - T/C \times 100$ where T and C represent tumor weights in IRT-treated (T) and untreated control (C) mice respectively. An IR of 58% was considered to represent an efficacious tumor response to IRT (17).

Histological Analysis

Intestinal cross-sections (4–6 μm) from each mouse were cut and stained with H&E, and intestinal micrometry was performed as described previously (15). The number of cells/hemi-crypt column and the number of surviving crypts/circumference were measured in both the small and large intestine at 12-h intervals ($n = 5$ mice/time point) after IRT administration as described previously (18, 19). Apoptotic cells within the small and large intestinal crypts were scored using the TUNEL assay and by their morphological appearance after staining with H&E. An apoptosis cell index was obtained on a positional basis for all intact half-crypts present in an entire jejunal and colonic cross-section per mouse, as described previously (20–22), 24 h after the first dose of IRT. Extensive crypt damage precluded an accurate positional analysis of apoptotic events beyond this time point. All slides were scored in a blinded fashion.

Microbiology

Aliquots of whole blood and tissue homogenates obtained using sterile technique were plated on blood agar plates and incubated at 37°C for 48 h.

Leukocyte Count. Whole blood samples were collected in venipuncture tubes containing EDTA and analyzed using an automated whole blood sorter calibrated for mouse samples. Blood smears were performed on all samples to confirm the automated analysis.

Immunoblotting. Intestinal lysates were centrifuged at 12,000 rpm for 30 min at 4°C and boiled for 5 min in sample buffer. Forty μgs of total protein were fractionated by discontinuous SDS-PAGE under reducing conditions and electrophoretically transferred onto Hybond-C nitrocellulose membrane (Amersham Pharmacia Biotech, Montreal, Canada) using standard techniques. Immunoreactive proteins were detected with a secondary antibody conjugated to horseradish peroxidase and an enhanced chemiluminescence commercial kit (Amersham Pharmacia Biotech) as described previously (23). Primary antibodies used included caspase-3 (1:5000 dilution; gift of R. Sekaly; Université de Montreal, Montreal, Canada), caspase-8 and caspase-9 (both at a 1:500 dilution; gift of T. Mak, University of Toronto, Toronto, Canada), p53 (1:500 dilution; Pab 246; Santa Cruz Biotechnology), PARP (1:4000 dilution; PharMingen, Mississauga, Ontario, Canada), and anti-actin (1:5000 dilution, Sigma). Densitometry was performed on blots exposed onto X-ray film (X-OMAT AR; Kodak Diagnostic Film) using a Hewlett Packard ScanJet 3p scanner and the NIH Image software.

Induction of Apoptosis in Transfected BHK Cells

BHK fibroblast cells containing the stably integrated pcDNA3.1 plasmid (BHK-pcDNA3; Invitrogen, Carlsbad, CA) or the identical plasmid containing the rat GLP-2 receptor (BHK-GLP-2R) were propagated as described previously (23). Cells were pretreated with either h[Gly2]-GLP-2 (20 nM) or forskolin (40 μM) before the addition of IRT (final concentration, 10 μM). Control cultures were treated identically in the absence of IRT, and the number of viable cells in each condition was measured using the Cell-Titer 96 aqueous assay kit (Promega, Madison, WI). Cells treated with IRT alone were fixed in 4% paraformaldehyde, and DNA was stained using 4′,6-diamidino-2-phenylindole (1 μg/ml; Sigma).

Measurement of Caspase-3-, Caspase-8-, and Caspase-9-like Enzymatic Activity

Enzymatic reactions were performed at 37°C using 150 μg of protein lysate, reaction buffer [50 mM HEPES (pH 7.4), 75 mM NaCl, 0.1% 3-[(3-cholamidopropyl)dimethylammonio]-1-propanesulfonic acid, and 2 mM DTT), and Ac-DEVD-pNA (Calbiochem, San Diego, CA) to measure caspase-3-like protease activity, Ac-IETD-pNA (Biosource International, Camarillo, CA) to measure caspase-8-like protease activity, and Ac-LEHD-pNA (Biosource International) to measure caspase-9-like protease activity. Spectrophotometric detection of the chromophore pNA at 405 nm was used to quantify enzymatic activity.

Statistical Analysis

Survival analysis was performed using the Fisher's exact t test. Statistical differences between treatment groups were determined by unpaired Student's t test or by ANOVA using n-1 *post hoc* custom hypotheses tests, as appropriate.

RESULTS

Administration of h[Gly2]-GLP-2 for 3 days before treatment with IRT significantly enhanced survival in CD1 mice (Fig. 1*A*). The protective effect of h[Gly2]-GLP-2 was not restricted to a single chemotherapeutic agent or murine genotype because h[Gly2]-GLP-2 significantly enhanced survival in BDF-1 mice after administration of the antimetabolite 5-FU (Fig. 1*B*).

To assess the efficacy of h[Gly2]-GLP-2 in tumor-bearing mice, CT-26 murine colon carcinoma tumor cells were injected into BALB/c mice and propagated *in vivo*. h[Gly2]-GLP-2 significantly enhanced survival after cyclical IRT administration to tumor-bearing mice (Fig. 1*C*, $P < 0.01$, h[Gly2]-GLP-2/IRT-treated mice *versus* all other groups of mice). Mice receiving both h[Gly2]-GLP-2 and IRT (100 mg/kg) tolerated three times the amount of IRT before mortality was observed (Fig. 1*C*). Furthermore, tumor-bearing mice given saline and IRT demonstrate progressive weight loss and lost 16% of their body weight over the entire duration of the experiment. Interestingly, h[Gly2]-GLP-2-treated mice demonstrated less weight loss between days 2–6 and 14–20 (data not shown; $P < 0.05$, mice treated with saline *versus* h[Gly2]-GLP-2 after IRT). Although h[Gly2]-GLP-2 enhanced survival and reduced weight loss, it did not impair IRT-induced tumor regression (Fig. 1*D*).

Because chemotherapy administration may be associated with increased intestinal permeability and bacterial septicemia, we assessed bacterial infection in chemotherapy-treated mice. h[Gly2]-GLP-2-treated mice exhibited a significant reduction in bacterial culture positivity in all organs examined 96 h after IRT administration (Fig. 2*A*, $P < 0.05$ for mice treated with saline *versus* h[Gly2]-GLP-2 after IRT). Furthermore, the bacterial burden (expressed as bacterial colonies/gram tissue) was significantly reduced in the liver and spleen (Fig. 2*B*, $P < 0.05$, mice treated with saline *versus* h[Gly2]-GLP-2 after IRT) and in the blood (Fig. 2*C*, $P < 0.05$, mice treated with saline *versus* h[Gly2]-GLP-2 after IRT) in h[Gly2]-GLP-2-treated mice. A significant leukopenia was observed in mice after IRT treatment, and the mean WBC count was modestly but significantly higher in h[Gly2]-GLP-2-treated mice (Fig. 2*D*).

To assess the histological consequences of h[Gly2]-GLP-2 action in the setting of chemotherapy, we analyzed the crypt compartment of IRT-treated mice. Morphometric analysis revealed a significant reduction in both the number of crypts and the number of cells within each crypt in the small and large intestine after IRT treatment (Fig. 3, *E*, *a–e*). h[Gly2]-GLP-2 significantly reduced the rate of crypt loss in the jejunum (Fig. 3*A*) and restored crypt cell number 96 h after IRT treatment (Fig. 3*B*). Similarly, h[Gly2]-GLP-2 pretreatment prevented crypt loss and enhanced the crypt cell number in the colon (Fig. 3, *C* and *D*).

To understand the mechanisms by which h[Gly2]-GLP-2 protected the crypt compartment of the small and large intestine from IRT-induced injury, a temporal and spatial analysis of apoptosis in the crypt compartment was performed. The number of apoptotic crypt

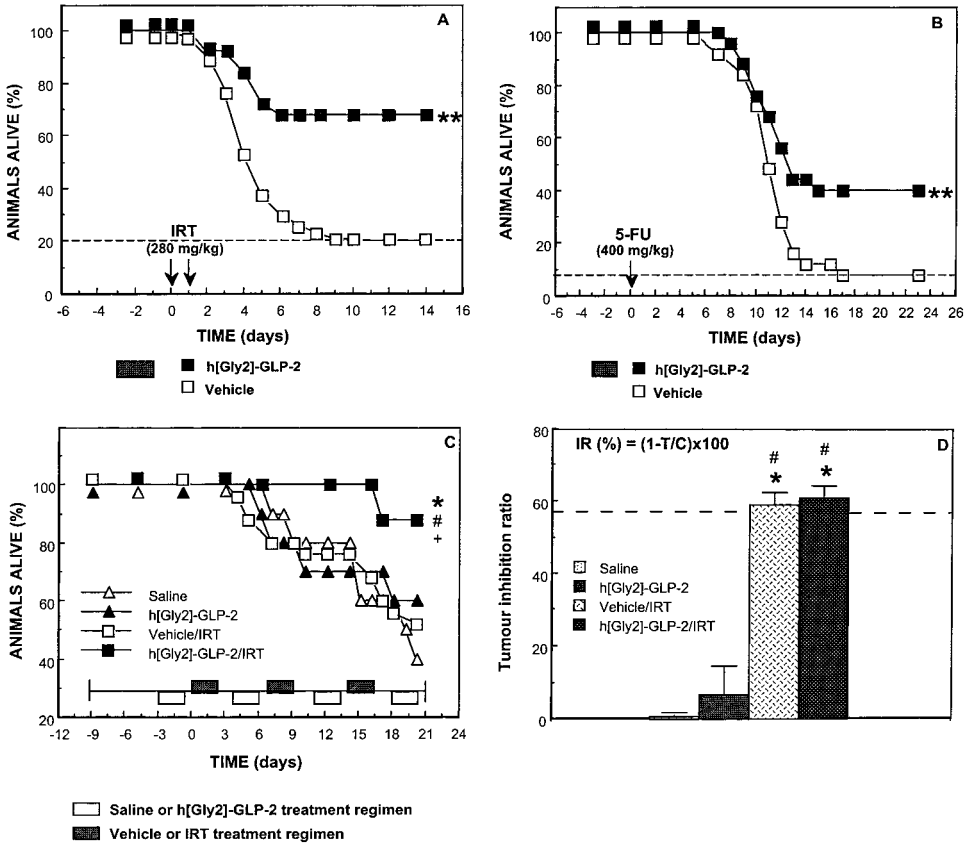

Fig. 1. Animal survival in (*A*) female CD1 mice treated with two doses of IRT, (*B*) female BDF1 mice treated with a single dose of 5-FU, and (*C*) female tumor-bearing BALB/c mice treated with IRT ($n = 25$ mice/treatment group). For experiments shown in *A* and *B*, mice were pretreated for 3 days with either saline or h[Gly2]-GLP-2 followed by administration of either two i.p. doses of IRT (*A*) or a single i.p. bolus of 5-FU (*B*). **, $P < 0.01$. *C*, repeated 7-day treatment regimens consisting of 3 days of either 0.5 ml of saline (PBS) or 10 μg of h[Gly2]-GLP-2 administered twice daily at 8 a.m. and 6 p.m., followed by 3 days of IRT (100 mg/kg dose) or vehicle administered once daily, followed by a 24-h recovery period. *, $P < 0.01$, saline- *versus* h[Gly2]-GLP-2/IRT-treated mice; #, $P < 0.01$, h[Gly2]-GLP-2- *versus* h[Gly2]-GLP-2/IRT-treated mice; +, $P < 0.01$, saline/IRT- *versus* h[Gly2]-GLP-2/IRT-treated mice). *D*, the tumor IR was determined as described previously (17). * and #, $P < 0.01$, IRT-treated *versus* non-IRT-treated groups.

cells was markedly increased after IRT treatment and significantly reduced in mice pretreated with h[Gly2]-GLP-2 (data not shown). Because pluripotent stem cells within the crypt compartment are thought to reside at cell positions 3–5 in the small intestine and 1–3 in the colon, whereas the clonogenic potential stem cells reside at positions 6–8 in the small intestine and 5–7 in the colon (21, 22), a positional topographical assessment of apoptosis within the crypt compartment was performed. h[Gly2]-GLP-2 pretreatment significantly reduced apoptosis in the jejunum at crypt cell positions 4–5 (Fig. 4*A*, $P < 0.05$, saline- *versus* h[Gly2]-GLP-2-treated mice). Similarly, h[Gly2]-GLP-2 reduced apoptosis in the colon at crypt cell positions 3–5, 7, and 8 (Fig. 4*B*, $P < 0.05$, saline- *versus* h[Gly2]-

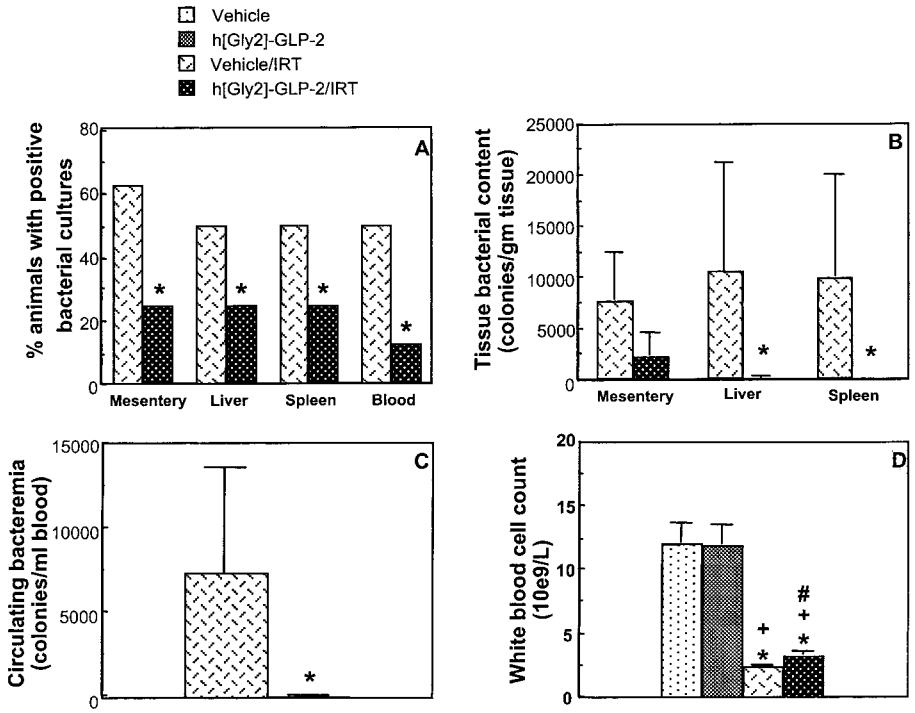

Fig. 2. *A*, prevalence of positive bacterial aerobic cultures from mesenteric, splenic, and liver homogenates and whole blood. Groups of mice ($n = 20$ mice/treatment group) were pretreated for 3 days with either saline or h[Gly2]-GLP-2 as shown in Fig. 1*A* and euthanized 96 h after commencing IRT treatment (two injections of 280 mg/kg/dose). *, $P < 0.05$ for saline- *versus* h[Gly2]-GLP-2-treated mice after IRT. No bacterial colonies were detected in homogenates from control mice ($n = 5$ mice/treatment group) treated with either saline or h[Gly2]-GLP-2 in the absence of IRT. Quantitative bacterial colony counts were obtained from mesenteric, splenic, and liver homogenates (*B*) and whole blood samples (*C*). *, $P < 0.05$, IRT-treated mice pretreated with saline *versus* h[Gly2]-GLP-2-treated mice. *D*, the leukocyte count in saline and h[Gly2]-GLP-2-treated control and IRT-treated mice. + and *, $P < 0.05$ for saline and h[Gly2]-GLP-2-treated groups *versus* IRT-treated mice. #, $P < 0.05$, IRT-treated mice pretreated with saline *versus* h[Gly2]-GLP-2-treated mice.

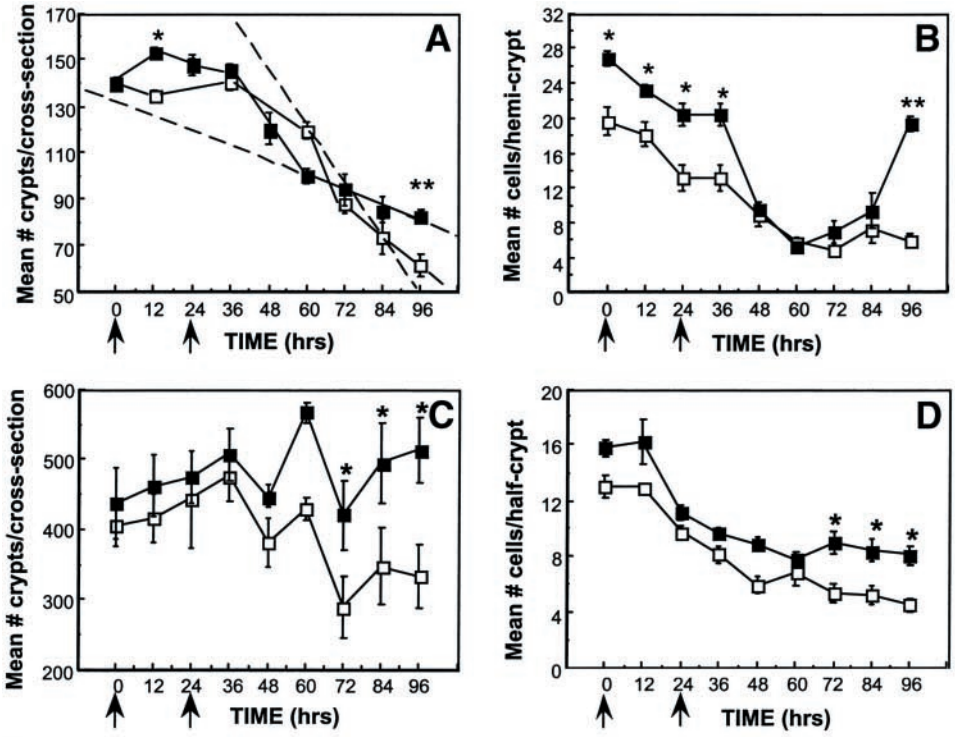

Fig. 3. Mean crypt survival (*A* and *C*) and mean cell number/hemi-crypt (*B* and *D*) from the midjejunum (*A* and *B*) and colon (*C* and *D*) of control and IRT-treated CD1 mice given saline (*Vehicle*) or h[Gly2]-GLP-2 as a 3-day pretreatment regimen. □, vehicle/IRT; ■, h[Gly2]-GLP-2/IRT. *Dashed lines* represent the line of best fit for data shown between 60 and 96 h. Five mice/treatment group were euthanized for analysis immediately before the first of two injections of IRT (280 mg/kg/dose) and at 12-h intervals up to 96 h. Crypt survival was measured along the entire bowel circumference, and the mean cell number/hemi-crypt was determined in 50 consecutive intact crypts/animal. *, $P < 0.05$; **, $P < 0.001$, saline- *versus* h[Gly2]-GLP-2 treated mice. *E*, photomicrographs of H&E-stained transverse intestinal sections from midjejunum. Saline (vehicle)-treated (*a–e*) and h[Gly2]-GLP-2-treated (*f–j*) CD1 mice before ($t = 0$ h) and 24, 48, 72, and 96 h after the first of two doses of IRT (280 mg/kg/dose). Magnification, ×400.

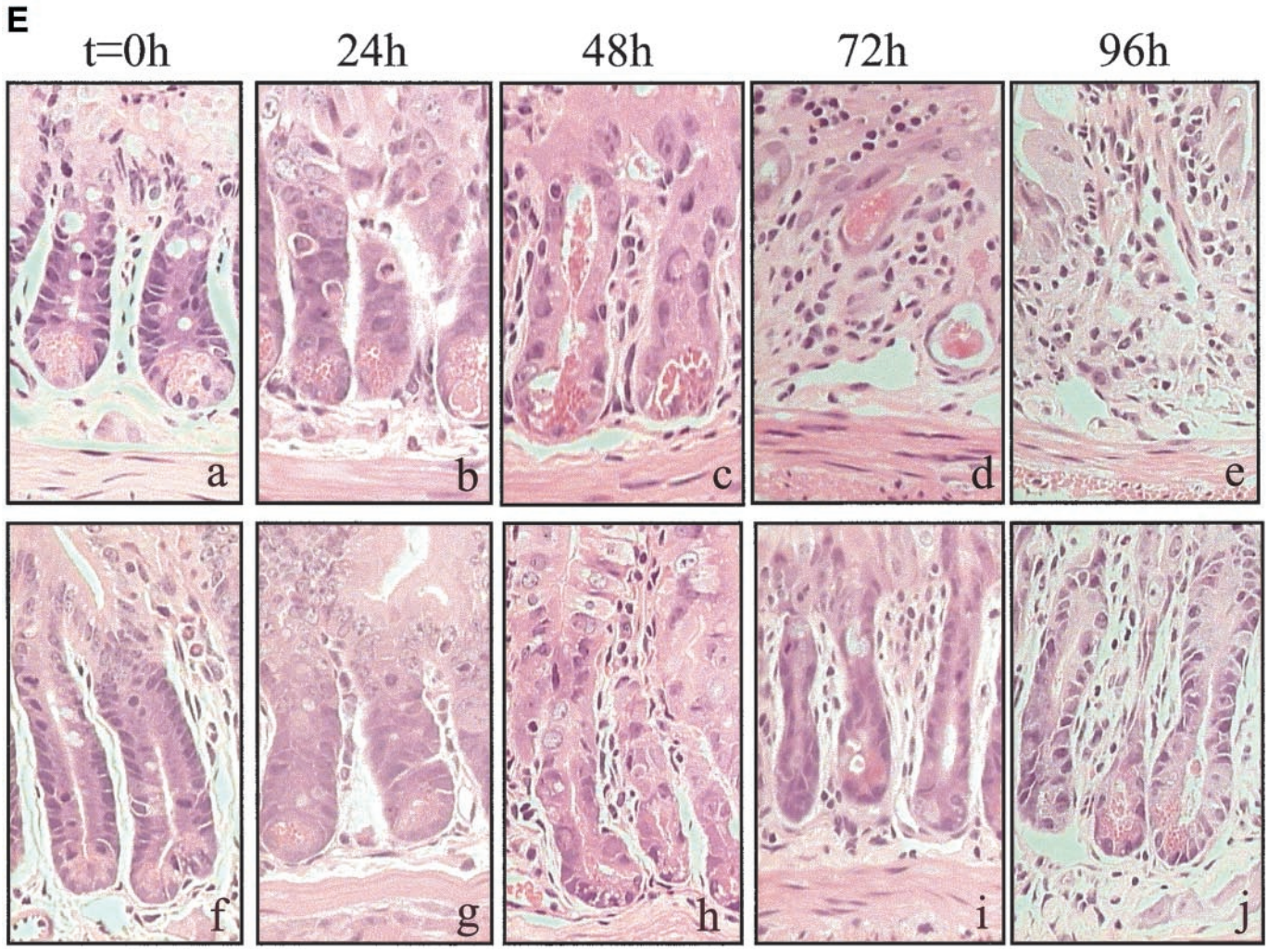

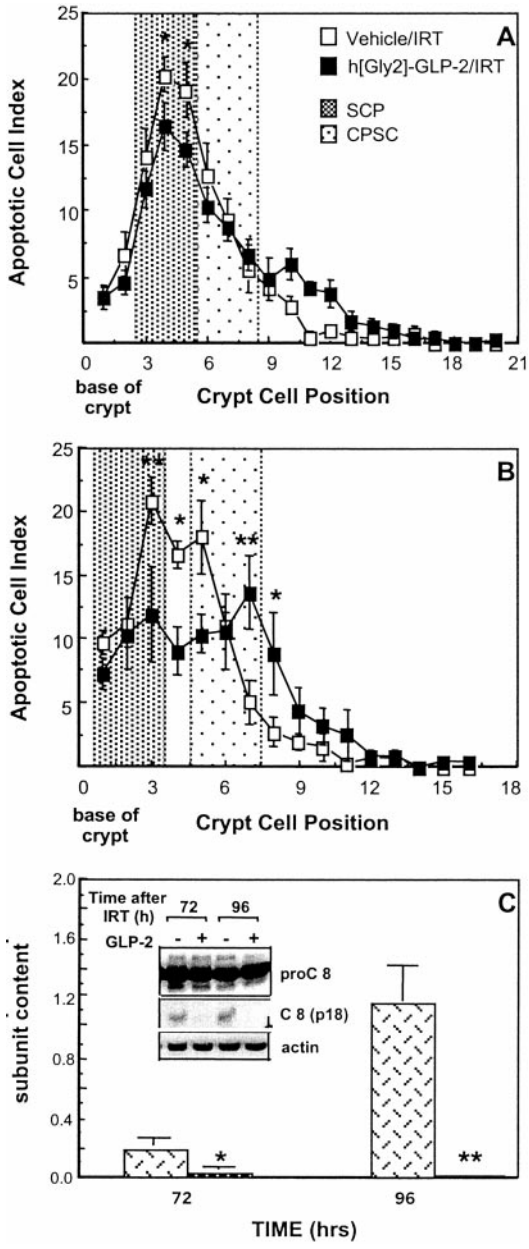

Fig. 4. Positional detection of apoptotic cells in the crypt compartment using the TUNEL assay. Apoptotic scores were determined from mid-jejunal (*A*) and colonic (*B*) intestinal crypt compartments of IRT-treated mice by determining the total number of TUNEL-positive cells in 50 continuous crypts ($n = 5$ animals/treatment group). *, $P < 0.05$; **, $P < 0.01$, saline *versus* h[Gly2]-GLP-2 treatment. Analysis was performed by calculating the percentage of TUNEL-positive cells in each crypt cell position for all intact crypts present in a single transverse intestinal cross-section, as described previously (20–22). Five mice/treatment group were analyzed at each time point. *, $P < 0.05$; **, $P < 0.01$, saline- *versus* h[Gly2]-GLP-2-treated mice. The stem cell region (*SCP*) and the clonogenic potential stem cell region (*CPSC*) are represented as indicated (20–22). *C*, analysis of procaspase-8 (*proC 8*) cleavage to the active p18 subunit (*C 8*) by Western blotting in the colon of mice after IRT treatment. *, $P < 0.05$; **, $P < 0.01$, vehicle *versus* h[Gly2]-GLP-2 treatment.

GLP-2-treated mice). Furthermore, a significant reduction in procaspase-8 cleavage was observed in the colon of h[Gly2]-GLP-2-treated mice at both 72 and 96 h after IRT treatment (Fig. 4*C*, $P < 0.05$ and $P < 0.01$ for saline- *versus* h[Gly2]-GLP-2-treated mice receiving IRT).

The small and large intestine is comprised of a mixed heterogeneous population of cell types that may be differentially affected by IRT. Because intestinal cell lines expressing the endogenous GLP-2 receptor have not yet been identified, we used BHK cells expressing the rat GLP-2 receptor (23) to examine the direct effects of GLP-2 on apoptosis *in vitro*. IRT induced apoptosis in BHK-GLP-2R cells as evidenced by detection of chromatin condensation and nuclear fragmentation (Fig. 5*A*). A significant improvement in cell viability was observed in BHK-GLP-2R cells but not control BHK cells after pretreatment with h[Gly2]-GLP-2 for 36 h before IRT administration (Fig. 5*B*). Analysis of caspase-8- and capase-9-like protease activity after IRT treatment was quantified by assessing cleavage of the substrates Ac-IETD-pNA and Ac-LEHD-pNA, respectively. h[Gly2]-GLP-2 treatment significantly reduced caspase-8-like enzymatic activity (Fig. 5*C*; $P < 0.05$). In contrast, h[Gly2]-GLP-2 had no effect on the levels of caspase-9-like enzymatic activity in IRT-treated cells (Fig. 5*C*). h[Gly2]-GLP-2 also reduced the IRT-induced cleavage of caspase-3 substrate Ac-DEVD-pNA and decreased procaspase-3 cleavage into the active p17 subunit (Fig. 5*D*). Furthermore, h[Gly2]-GLP-2 also decreased the IRT-induced cleavage of PARP, a downstream substrate of activated caspase-3 (Fig. 5*E*).

DISCUSSION

IRT hydrochloride, a potent DNA topoisomerase I inhibitor, is active against a broad variety of hematological and gastrointestinal neoplasms and induces apoptosis in both normal and neoplastic cell types (24, 25). Furthermore, IRT produces extensive intestinal toxicity that is manifested histologically as mucositis and clinically as both early- and late-onset diarrhea in both human (2, 26) and rodent studies (27, 28). Our results demonstrate that administration of h[Gly2]-GLP-2 significantly improves survival, reduces bacterial infection, and decreases intestinal damage in IRT-treated mice. The protective effects of h[Gly2]-GLP-2 are not restricted to a single class of chemotherapeutic agent because h[Gly2]-GLP-2 significantly increased survival in 5-FU-treated animals. Furthermore, h[Gly2]-GLP-2 also improves survival and reduces weight loss in IRT-treated tumor-bearing mice, demonstrating that the protective effects of GLP-2 are not diminished in the setting of active neoplasia.

The significant reduction in chemotherapy-associated mortality in h[Gly2]-GLP-2-treated mice may be explained in part by the reduction in circulating bacteremia. Recent experiments have demonstrated that GLP-2 reduces mucosal permeability in rats after major small bowel resection (29). Furthermore, GLP-2 markedly reduced circulating bacteremia and decreased bacterial infection in the liver and spleen in mice after indomethacin-induced intestinal injury (15). Although the precise mechanism(s) activated by h[Gly2]-GLP-2 leading to reduction in bacterial infection remains unknown, the demonstration that h[Gly2]-GLP-2 reduced macromolecule flux, decreased intestinal permeability, and markedly enhanced intestinal barrier function in GLP-2-treated mice (30) provides a clear link between GLP-2 action and reduced bacterial translocation in the setting of intestinal injury. Hence, it seems likely that GLP-2-mediated enhancement of intestinal barrier function contributes to the reduction in bacterial sepsis observed after IRT administration in h[Gly2]-GLP-2-treated mice.

The initial observation that GLP-2 exerts trophic actions in the intestinal mucosa was largely attributed to stimulation of crypt cell proliferation (11, 14). Although the number of identifiable cells undergoing spontaneous apoptosis in the normal intestinal crypt compartment is low, intestinal injury after exposure to ionizing radiation or chemical agents results in marked induction of apoptosis in the crypt compartment (6–8, 20–22, 31, 32). Our finding that GLP-2 reduces the percentage of apoptotic cells in the crypt compartment after chemotherapy is consistent with recent evidence demonstrating a marked reduction in crypt apoptosis after GLP-2 treatment of mice

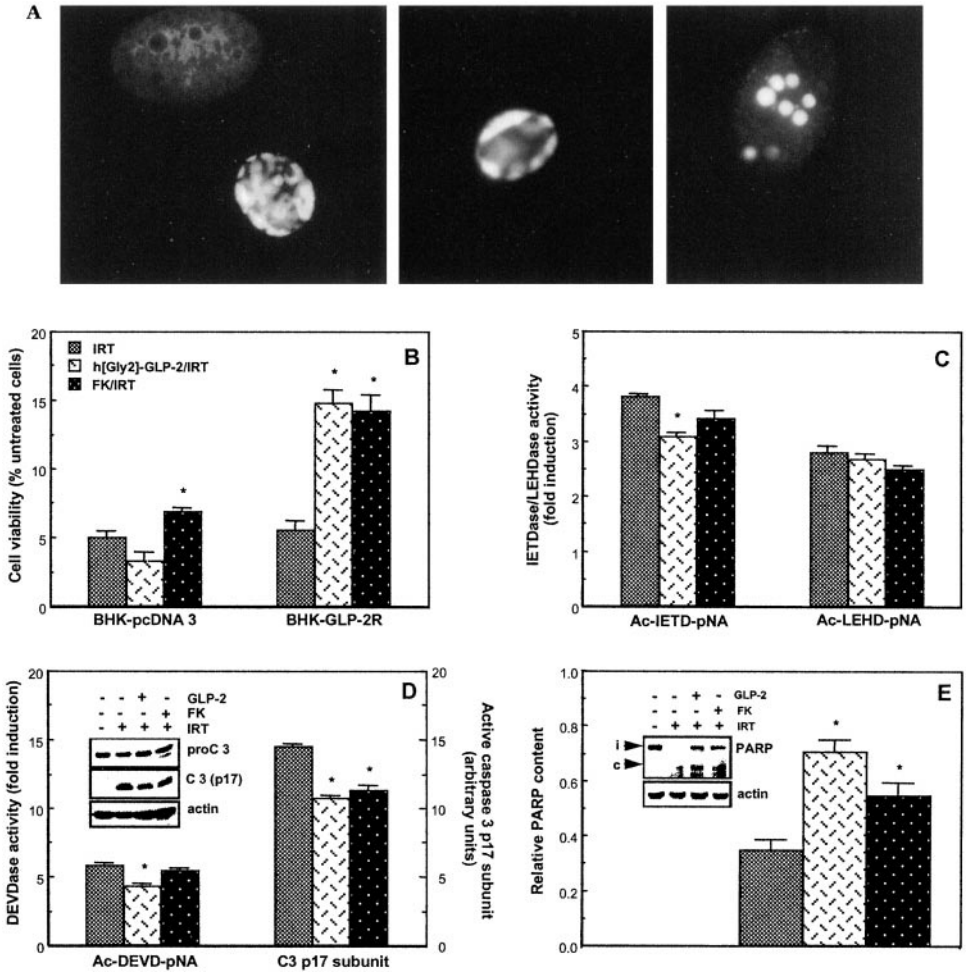

Fig. 5. IRT induced apoptosis in a BHK fibroblast cell line containing the stably integrated pcDNA3.1 plasmid (*BHK-pcDNA3*) or the identical plasmid directing expression of the rat GLP-2 receptor (*BHK-GLP-2R*). *A*, fluorescent microscopic visualization of chromatin condensation and nuclear fragmentation in BHK-GLP-2R cells 24 h after IRT administration, as demonstrated by 4′,6-diamidino-2-phenylindole nuclear staining. *B*, analysis of cell viability in BHK-pcDNA3 and BHK-GLP-2R cells, respectively, after IRT treatment. Values are derived from experiments performed in quadruplicate. ∗, $P < 0.05$, IRT alone *versus* IRT/h[Gly2]-GLP-2. *C*, analysis of caspase-like activity in BHK-GLP-2R cells after treatment with IRT. Ac-IETD-pNA (caspase-8-like activity) and Ac-LEHD-pNA (caspase-9-like activity) are represented as fold induction compared with cells that were not treated with IRT. ∗, $P < 0.05$, h[Gly2]-GLP-2/IRT *versus* IRT. *D*, cleavage of Ac-DEVD-pNA (caspase-3-like enzyme activity) and procaspase-3 in IRT-treated cells treated with or without h[Gly2]-GLP-2 or forskolin (*Fk*). ∗, $P < 0.01$, vehicle-treated cells *versus* forskolin- or h[Gly2]-GLP-2-treated cells. *E*, Western blot analysis of PARP cleavage in IRT-treated BHK-GLP-2R cells. ∗, $P < 0.05$ for IRT alone *versus* IRT/forskolin or IRT/h[Gly2]-GLP-2. For data in *C–E*, values are expressed as fold induction relative to untreated cells. The relative densitometric values for caspase-3 (*D*) or PARP (*E*) were normalized to the values obtained for actin in the same experiments and represent the means of three to four separate experiments.

with indomethacin-induced enteritis (15). Hence, the available evidence suggests that GLP-2 maintains the integrity of the intestinal epithelium by both stimulating cell proliferation and inhibiting apoptotic cell death in the crypt compartment.

What are the mechanisms activated by GLP-2 signaling that confer resistance to apoptosis-mediated injury in the intestinal epithelium after IRT treatment? Consistent with studies demonstrating the importance of the CPP32 subfamily of caspases in the pathogenesis of IRT-induced apoptosis (24), we observed reduced IRT-mediated caspase-3 and PARP activation in BHK-GLP-2R cells after GLP-2 treatment *in vitro*. Furthermore, a significant reduction of procaspase-8 cleavage, as evidenced by inhibition of p18 subunit generation, was observed in GLP-2-treated intestine after IRT administration *in vivo*. In contrast, we did not observe any changes in the levels of caspase-9 after GLP-2 treatment of mice *in vivo* or of cells *in vitro*. These findings, summarized in Fig. 6, demonstrate for the first time that GLP-2 receptor signaling may be linked directly to specific cell survival pathways in heterologous cell types.

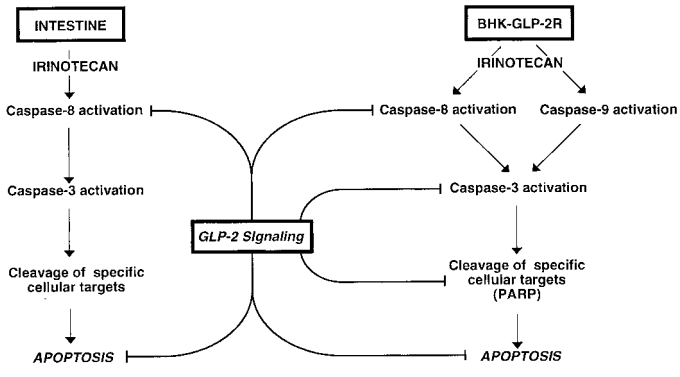

Fig. 6. Schematic representation of how GLP-2R-dependent signaling regulates IRT-induced apoptosis in the intestine *in vivo* and in cells expressing the transfected GLP-2 receptor (*BHK-GLP-2R*) *in vitro*.

Although signaling through G protein-coupled receptors of the glucagon/GLP-1/GLP-2 receptor superfamily has not previously been reported to modify apoptotic pathways, recent experiments suggest an emerging link between G protein-coupled receptor signaling and cell death. Activation of the somatostatin receptor modulates pH-dependent cell death in heterologous cell types (33, 34), and signaling through the parathyroid hormone/parathyroid hormone-related protein receptor diminishes activation of apoptotic pathways in cells of the chondrocyte and osteoblast lineages (35). Although the cellular localization of intestinal GLP-2 receptor expression has not yet been identified, our data clearly suggest that intestinal cells expressing the GLP-2R are likely to be protected from cell death associated with exposure to genotoxic stress *in vivo*. Given the emerging importance of GLP-2 receptor signaling for preservation of intestinal mucosa in the face of external injury (15, 29, 36, 37), our findings provide a scientific rationale for exploring the therapeutic use of GLP-2 in settings characterized by induction of intestinal injury via activation of apoptosis in the mucosal epithelium *in vivo*.

REFERENCES

1. Wadler, S., Benson, A. B., III, Engelking, C., Catalano, R., Field, M., Kornblau, S. M., Mitchell, E., Rubin, J., Trotta, P., and Vokes, E. Recommended guidelines for the treatment of chemotherapy-induced diarrhea. J. Clin. Oncol., *16:* 3169–3178, 1998.
2. Van Huyen, J. P., Bloch, F., Attar, A., Levoir, D., Kreft, C., Molina, T., and Bruneval, P. Diffuse mucosal damage in the large intestine associated with irinotecan (CPT-11). Dig. Dis. Sci., *43:* 2649–2651, 1998.
3. Dombret, H., Chastang, C., Fenaux, P., Reiffers, J., Bordessoule, D., Bouabdallah, R., Mandelli, F., Ferrant, A., Auzanneau, G., Tilly, H., *et al.* A controlled study of recombinant human granulocyte colony-stimulating factor in elderly patients after treatment for acute myelogenous leukemia. AML Cooperative Study Group. N. Engl. J. Med., *332:* 1678–1683, 1995.
4. Taupin, D. R., Kinoshita, K., and Podolsky, D. K. Intestinal trefoil factor confers colonic epithelial resistance to apoptosis. Proc. Natl. Acad. Sci. USA, *97:* 799–804, 2000.
5. Mashimo, H., Wu, D-C., Podolsky, D. K., and Fishman, M. C. Impaired defense of intestinal mucosa in mice lacking intestinal trefoil factor. Science (Washington DC), *274:* 262–265, 1996.
6. Farrell, C. L., Bready, J. V., Rex, K. L., Chen, J. N., DiPalma, C. R., Whitcomb, K. L., Yin, S., Hill, D. C., Wiemann, B., Starnes, C. O., Havill, A. M., Lu, Z. N., Aukerman, S. L., Pierce, G. F., Thomason, A., Potten, C. S., Ulich, T. R., and Lacey, D. L. Keratinocyte growth factor protects mice from chemotherapy and radiation-induced gastrointestinal injury and mortality. Cancer Res., *58:* 933–939, 1998.
7. Houchen, C. W., George, R. J., Sturmoski, M. A., and Cohn, S. M. FGF-2 enhances intestinal stem cell survival and its expression is induced after radiation injury. Am. J. Physiol., *276:* G249—G258, 1999.
8. Cao, S., Black, J. D., Troutt, A. B., and Rustum, Y. M. Interleukin 15 offers selective protection from irinotecan-induced intestinal toxicity in a preclinical animal model. Cancer Res., *58:* 3270–3274, 1998.
9. Orazi, A., Du, X., Yang, Z., Kashai, M., and Williams, D. A. Interleukin-11 prevents apoptosis and accelerates recovery of small intestinal mucosa in mice treated with combined chemotherapy and radiation. Lab. Investig., *75:* 33–42, 1996.
10. McCormack, E. S., Borzillo, G. V., Ambrosino, C., Mak, G., Hamablet, L., Qu, G. Y., and Haley, J. D. Transforming growth factor-β3 protection of epithelial cells from cycle-selective chemotherapy *in vitro*. Biochem. Pharmacol., *53:* 1149–1159, 1997.
11. Drucker, D. J., Ehrlich, P., Asa, S. L., and Brubaker, P. L. Induction of intestinal epithelial proliferation by glucagon-like peptide 2. Proc. Natl. Acad. Sci. USA, *93:* 7911–7916, 1996.
12. Drucker, D. J., Shi, Q., Crivici, A., Sumner-Smith, M., Tavares, W., Hill, M., Deforest, L., Cooper, S., and Brubaker, P. L. Regulation of the biological activity of glucagon-like peptide 2 by dipeptidyl peptidase IV. Nat. Biotechnol., *15:* 673–677, 1997.
13. Drucker, D. J. The glucagon-like peptides. Diabetes, *47:* 159–169, 1998.
14. Tsai, C-H., Hill, M., Asa, S. L., Brubaker, P. L., and Drucker, D. J. Intestinal growth-promoting properties of glucagon-like peptide 2 in mice. Am. J. Physiol., *273:* E77–E84, 1997.
15. Boushey, R. P., Yusta, B., and Drucker, D. J. Glucagon-like peptide 2 decreases mortality and reduces the severity of indomethacin-induced murine enteritis. Am. J. Physiol., *277:* E937–E947, 1999.
16. Shinohara, H., Killion, J. J., Kuniyasu, H., Kumar, R., and Fidler, I. J. Prevention of intestinal toxic effects and intensification of irinotecan's therapeutic efficacy against murine colon cancer liver metastases by oral administration of the lipopeptide JBT 3002. Clin. Cancer Res., *4:* 2053–2063, 1998.
17. Kunimoto, T., Nitta, K., Tanaka, T., Uehara, N., Baba, H., Takeuchi, M., Yokokura, T., Sawada, S., Miyasaka, T., and Mutai, M. Antitumor activity of 7-ethyl-10-[4-(1-piperidino)-1- piperidino]carbonyloxy-camptothecin, a novel water-soluble derivative of camptothecin, against murine tumors. Cancer Res., *47:* 5944–5947, 1987.
18. Wright, N. A., Carter, J., and Irwin, M. The measurement of villus cell population size in the mouse small intestine in normal and abnormal states: a comparison of absolute measurements with morphometric estimators in sectioned immersion-fixed material. Cell Tissue Kinet., *22:* 425–450, 1989.
19. Withers, H. R., and Elkind, M. M. Microcolony survival assay for cells of mouse intestinal mucosa exposed to radiation. Int. J. Radiat. Biol. Relat. Stud. Phys. Chem. Med., *17:* 261–267, 1970.
20. Pritchard, D. M., Potten, C. S., and Hickman, J. A. The relationships between p53-dependent apoptosis, inhibition of proliferation, and 5-fluorouracil-induced histopathology in murine intestinal epithelia. Cancer Res., *58:* 5453–5465, 1998.
21. Potten, C. S., and Grant, H. K. The relationship between ionizing radiation-induced apoptosis and stem cells in the small and large intestine. Br. J. Cancer, *78:* 993–1003, 1998.
22. Ijiri, K., and Potten, C. S. Response of intestinal cells of differing topographical and hierarchical status to ten cytotoxic drugs and five sources of radiation. Br. J. Cancer, *47:* 175–185, 1983.
23. Yusta, B., Somwar, R., Wang, F., Munroe, D., Grinstein, S., Klip, A., and Drucker, D. J. Identification of glucagon-like peptide-2 (GLP-2)-activated signaling pathways in baby hamster kidney fibroblasts expressing the rat GLP-2 receptor. J. Biol. Chem., *274:* 30459–30467, 1999.
24. Suzuki, A., Iwasaki, M., Kato, M., and Wagai, N. Sequential operation of ceramide synthesis and ICE cascade in CPT-11-initiated apoptotic death signaling. Exp. Cell Res., *233:* 41–47, 1997.
25. Walton, M. I., Whysong, D., O'Connor, P. M., Hockenbery, D., Korsmeyer, S. J., and Kohn, K. W. Constitutive expression of human Bcl-2 modulates nitrogen mustard and camptothecin induced apoptosis. Cancer Res., *53:* 1853–1861, 1993.
26. Boland, C. R., Sinicrope, F. A., Brenner, D. E., and Carethers, J. M. Colorectal cancer prevention and treatment. Gastroenterology, *118:* S115–S128, 2000.
27. Thompson, J., Stewart, C. F., and Houghton, P. J. Animal models for studying the action of topoisomerase I targeted drugs. Biochim. Biophys. Acta, *1400:* 301–319, 1998.
28. Ikuno, N., Soda, H., Watanabe, M., and Oka, M. Irinotecan (CPT-11) and characteristic mucosal changes in the mouse ileum and cecum. J. Natl. Cancer Inst., *87:* 1876–1883, 1995.
29. Scott, R. B., Kirk, D., MacNaughton, W. K., and Meddings, J. B. GLP-2 augments the adaptive response to massive intestinal resection in rat. Am. J. Physiol, *275:* G911–G921, 1998.
30. Benjamin, M. A., McKay, D. M., Yang, P-C., and Perdue, M. H. Glucagon-like peptide-2 enhances epithelial barrier function of both transcellular and paracellular pathways in the mouse. Gut, *47:* 112–119, 2000.
31. Coopersmith, C. M., and Gordon, J. I. γ-Ray-induced apoptosis in transgenic mice with proliferative abnormalities in their intestinal epithelium: re-entry of villus enterocytes into the cell cycle does not affect their radioresistance but enhances the radiosensitivity of the crypt by inducing p53. Oncogene, *15:* 131–141, 1997.
32. Watson, A. J., and Pritchard, D. M. VII. Apoptosis in intestinal epithelium: lessons from transgenic and knockout mice. Am. J. Physiol Gastrointest. Liver Physiol., *278:* G1–G5, 2000.
33. Thangaraju, M., Sharma, K., Liu, D., Shen, S. H., and Srikant, C. B. Interdependent regulation of intracellular acidification and SHP-1 in apoptosis. Cancer Res., *59:* 1649–1654, 1999.
34. Sharma, K., Patel, Y. C., and Srikant, C. B. C-terminal region of human somatostatin receptor 5 is required for induction of Rb and G_1 cell cycle arrest. Mol. Endocrinol., *13:* 82–90, 1999.
35. Turner, P. R., Mefford, S., Christakos, S., and Nissenson, R. A. Apoptosis mediated by activation of the G protein-coupled receptor for parathyroid hormone (PTH)/PTH-related protein (PTHrP). Mol. Endocrinol., *14:* 241–254, 2000.
36. Drucker, D. J., Yusta, B., Boushey, R. P., Deforest, L., and Brubaker, P. L. Human [Gly2]-GLP-2 reduces the severity of colonic injury in a murine model of experimental colitis. Am. J. Physiol., *276:* G79–G91, 1999.
37. Prasad, R., Alavi, K., and Schwartz, M. Z. Glucagonlike peptide-2 analogue enhances intestinal mucosal mass after ischemia and reperfusion. J. Pediatr. Surg., *35:* 357–359, 2000.